NASA TECHNICAL NOTE

NASA TN D-3698

c. 1

NASA TN D-3698

SOME EFFECTS OF JET PLUMING ON THE STATIC STABILITY OF BALLISTIC BODIES AT A MACH NUMBER OF 6.00

by Robert J. McGhee

Langley Research Center
Langley Station, Hampton, Va.

NATIONAL AERONAUTICS AND SPACE ADMINISTRATION • WASHINGTON, D. C. • NOVEMBER 1966

SOME EFFECTS OF JET PLUMING ON THE STATIC STABILITY OF BALLISTIC BODIES AT A MACH NUMBER OF 6.00

By Robert J. McGhee

Langley Research Center
Langley Station, Hampton, Va.

NATIONAL AERONAUTICS AND SPACE ADMINISTRATION

For sale by the Clearinghouse for Federal Scientific and Technical Information
Springfield, Virginia 22151 – Price $2.00

SOME EFFECTS OF JET PLUMING ON THE STATIC STABILITY OF BALLISTIC BODIES AT A MACH NUMBER OF 6.00

By Robert J. McGhee
Langley Research Center

SUMMARY

An investigation has been conducted in a 2-foot hypersonic facility at the Langley Research Center at a Mach number of 6.00 to determine some effects of jet pluming on the static stability of ballistic bodies. Effects of forebody and afterbody geometry as well as fins and flares were investigated. The ratio of jet pressure to free-stream static pressure ranged from jet-off conditions to about 7000. The model angle of attack varied from -2° to 8°. Test Reynolds number based on body diameter was approximately 0.07×10^{6}.

The results indicate that increasing the jet-pressure ratio resulted in shock-induced separation which was accompanied by significant decreases in both normal-force-curve slopes and static stability. Increasing the angle of attack resulted in the stabilizing surfaces recovering a large measure of their effectiveness with corresponding increases in stability; however, for large jet-pressure ratios little or no improvement resulted at the highest angle of attack. For the 30° (half-angle) conical forebody and flare afterbody, increasing the length of the centerbody resulted in a decrease in the jet-plume-induced destabilizing contribution. For any forebody, the finned afterbody reduced the variations in center of pressure to about 1 body diameter for the entire range of jet-pressure ratios. Changes in center of pressure were more abrupt in the low jet-pressure-ratio range for either the cylindrical or flared afterbody compared with changes for the finned afterbody.

INTRODUCTION

An underexpanded rocket nozzle may have important effects on aerodynamic stability and control of rocket vehicles. When the ratio of jet-exit pressure to ambient static pressure becomes sufficiently large (gross underexpansion), the hot exhausting jet will expand to form a large plume at the base of the vehicle. This plume in turn may cause extensive boundary-layer separation on the vehicle surfaces forward of the nozzle exit. Examples of such separation are shown in references 1 and 2. The jet-plume-induced separated boundary layer can be expected to degrade aerodynamic stability as

well as control, since the aerodynamic surfaces such as fins or flares may lie entirely within the separated regions.

Investigations of this phenomenon have been reported in references 1 to 4; however, most of the results are for low ratios of jet-exit pressure to ambient static pressure. The present investigation was therefore initiated to study the jet-plume effects on static stability at high ratios of jet-exit to ambient static pressure. The investigation included some of the effects of forebody and afterbody geometry as well as fins and flares on static stability in the presence of a gaseous jet boundary. Normal force and pitching moment were measured for the models in such a manner that only exhaust-plume-induced body forces and moments were measured. A supersonic exhaust nozzle was used with compressed gaseous nitrogen to simulate the jet plume.

The investigation was conducted in a 2-foot hypersonic facility at the Langley Research Center at a Mach number of 6.00. The ratio of the jet pressure to free-stream static pressure ranged from jet-off conditions to about 7000. The model angle of attack was varied from -2° to 8°. Test Reynolds number based on body diameter was approximately 0.07×10^{6}.

SYMBOLS

The aerodynamic data are reduced to coefficient form and referred to the body axes. The moment reference for all data was 3.22 body diameters forward of the model base. The units used for the physical quantities defined are given in the International System of Units (SI).

A cross-sectional area of cylinder, 7.246 centimeters^2

d diameter of cylinder, 3.038 centimeters

C_N normal-force coefficient, $\dfrac{\text{Normal force}}{q_\infty A}$

C_m pitching-moment coefficient, $\dfrac{\text{Pitching moment}}{q_\infty A d}$

q_∞ free-stream dynamic pressure, newtons per meter^2

p_j/p_∞ jet-pressure ratio (ratio of jet-exit to free-stream static pressure)

x_{cp}/d center-of-pressure location forward of model base

x,y rectangular coordinates (fig. 3)

α angle of attack, degrees

MODELS AND TESTS

Models

A photograph of each model tested and its designation are shown in figure 1 and a general arrangement of a typical model is shown in figure 2. The configuration designations are identified in table I. Each configuration consisted of a forebody (first digit in designation), cylindrical centerbody (second digit), and an afterbody (third digit). Details of the model components and supersonic nozzle are presented in figures 3 and 4, respectively.

The forebodies (fig. 3) consisted of a 30° half-angle cone, a 15° half-angle cone, and an ogive with a nose radius of 0.1 cm. The afterbodies consisted of a fin with a 30° sweptback leading edge, a 20° flare, and a straight cylinder. Most of the tests were conducted with a short cylindrical centerbody having a length-diameter ratio of 2.84; however, the 30° conical forebody with the flare afterbody was tested with a long cylindrical centerbody having a length-diameter ratio of 7.02.

The model support sting, a hollow steel tube, allowed the gaseous nitrogen from the supply tank to be emptied into the settling chamber of the nozzle through four louvers. (See fig. 2.) The supersonic nozzle was designed as an annular nozzle because only the outer boundary of the plume requires simulation and because the model required a sting mount. The nozzle had an area ratio of 2.07 (exit area to throat area) and the nozzle divergence angle ($17^{\circ}57'$) approximated that for a representative rocket engine. Cold gaseous nitrogen at approximately local atmospheric temperature was used to simulate the exhaust plume. Allowance was made in the nozzle design for the presence of the center support sting.

Instrumentation

A two-component strain-gage balance was used to measure normal force and pitching moment. The pressure in the model settling chamber was measured with a Bourdon pressure gage which was visually monitored during the tests. Schlieren data were obtained with a 2-msec flash synchronized to a 40-frame/sec movie camera in order to observe the flow behavior.

Tests and Accuracy

This investigation was conducted in a 2-foot hypersonic facility at the Langley Research Center, described in reference 5, at a Mach number of 6.00. The angle-of-attack range was from -2° to 8° and the jet-exit to free-stream static pressure ratio was varied from jet-off conditions to about 7000. The flow over the models was considered to be essentially laminar with the exception of configuration 122 (long centerbody) where transition to turbulent flow may have occurred. Reynolds number based on body diameter was approximately 0.07×10^6.

Jet-pressure ratios p_j/p_∞ are estimated to be accurate within ± 2 percent. Test Mach number variation was within ± 0.02. Angle of attack was corrected for balance and sting bending and is believed to be accurate to within $\pm 0.20^{\circ}$. The estimated accuracy of C_m and C_N based on balance accuracy and repeatability is ± 0.04.

RESULTS AND DISCUSSION

The results of this investigation have been divided into two parts: the effects of jet-pressure ratio and angle of attack and the variation of the center of pressure with jet-pressure ratio. Figures 5 to 12 present the variation of C_N and C_m with angle of attack and jet-pressure ratio for all configurations and representative schlieren photographs for most configurations. Figure 13 presents the variation of center-of-pressure location with jet-pressure ratio at $\alpha = 0^{\circ}$ for the configurations tested.

Effect of Jet-Pressure Ratio and Angle of Attack

Figures 5 to 11 show that at jet-off conditions both C_N and C_m were essentially linear with angle of attack at small angles. As p_j/p_∞ was increased, a large billowing jet plume was formed (see fig. 5(b)) and resulted in shock-induced separation over at least the rearward portions of the models. Substantial decreases in normal force and corresponding destabilizing pitching moments throughout the angle-of-attack range were measured for all jet-on conditions. It should be observed that the lowest pressure ratio was about 550; however, a minimum pressure ratio of about 100 was indicated by reference 2 as the pressure ratio at which jet-plume-induced separated flow was first observed.

In the low angle-of-attack range (0° to 2°), for values of p_j/p_∞ greater than about 550, the separation point moved for both conical forebodies to the forebody-cylinder juncture (figs. 5, 6, 7, and 9) and the afterbodies were partially or completely immersed in separated flow. Increases in p_j/p_∞ generally caused the cone angle of the separated flow to increase. For the cylindrical afterbody (fig. 5), increasing jet-pressure ratio did not cause appreciable changes in C_m after the separation had once occurred; however,

for all configurations employing fins or flares, increases in p_j/p_∞ resulted in a decrease in stability up to values of p_j/p_∞ of about 1500. Beyond this value further increases had little effect on stability changes.

As the angle of attack was increased (2^o to 8^o) the jet plume was compressed on the windward side of the models. Eventually some flow reattachment occurred or at least the stabilizing surfaces recovered a large measure of their effectiveness with corresponding increases in both normal-force-curve slope and stability. The angle of attack at which reattachment occurred increased with increasing p_j/p_∞; only small stability recovery occurred at the highest values of p_j/p_∞.

In figure 12 the effect of the short centerbody is compared with that of the long centerbody for the configuration which employed the 30^o conical forebody and the flare afterbody. Only jet-off data and data for a jet-pressure ratio of about 3400 are shown. Aside from the unstable contributions expected from the long centerbody, the principal effect of changing the length is that the jet-plume-induced destabilizing contribution to the moments, as well as the change in normal-force-curve slope, was small for the long centerbody. A suitable explanation for the reduced plume influence cannot be obtained from the available data. A possible explanation may lie in the differences in Reynolds number, especially if transition to turbulent flow actually occurred on the long body.

Center-of-Pressure Variation

Figure 13 shows, at jet-off conditions, that the flare is more effective than the fin in stabilizing the models. Forebody-shape changes did not produce a substantial change of the jet-off center of pressure for the same afterbody; however, the 30^o conical forebody exhibited a center of pressure estimated to lie about 0.5d forward of that for either the 15^o conical or the ogive forebody.

For the jet on, figure 13 shows that, with the cylindrical afterbody, the variation of center of pressure with jet-pressure ratio was abrupt and exceeded 9 body diameters, nearly all of which occurred between jet-off condition and $p_j/p_\infty \approx 3500$. The finned afterbody, with any of the forebodies, reduced the variations in center of pressure to only about 1 body diameter for the entire range of jet-pressure ratios from 550 to about 6700. These shifts occurred gradually with increasing pressure ratio. The variation of center of pressure with increasing jet-pressure ratio for the flared afterbody was similar to that for the cylindrical afterbody, that is, it was abrupt but only about half as much or about 5 diameters. For the 30^o conical forebody, all the shifts occurred below $p_j/p_\infty \approx 1500$; however, for the 15^o conical or the ogive forebody, most of the shifts occurred below $p_j/p_\infty \approx 700$.

CONCLUDING REMARKS

An investigation has been conducted in a 2-foot hypersonic facility at the Langley Research Center at a Mach number of 6.00 to determine some effects of jet pluming on the static stability of ballistic bodies. The ratio of jet pressure to free-stream static pressure ranged from jet-off conditions to about 7000. The model angle of attack varied from -2° to 8°. Test Reynolds number based on body diameter was approximately 0.07×10^{6}. The principal results may be summarized as follows:

1. Increasing the jet-pressure ratio resulted in shock-induced separation which was accompanied by significant decreases in normal-force-curve slopes and decreased the static stability.

2. Increasing the angle of attack resulted in the stabilizing surfaces recovering a large measure of their effectiveness with corresponding increases in stability; however, for large jet-pressure ratios little or no improvement resulted at the highest angle of attack of these tests.

3. For the 30° (half-angle) conical forebody and flare afterbody, increasing the length of the centerbody resulted in a decrease in the jet-plume-induced destabilizing contribution.

4. For any forebody, the finned afterbody reduced the variations in center of pressure to about 1 body diameter for the entire range of jet-pressure ratios.

5. Changes in center of pressure were more abrupt in the low jet-pressure-ratio range for either the cylindrical or flared afterbody compared with changes for the finned afterbody.

Langley Research Center,
National Aeronautics and Space Administration,
Langley Station, Hampton, Va., July 20, 1966,
128-31-06-05-23.

REFERENCES

1. Salmi, Reino J.: Effects of Jet Billowing on Stability of Missile-Type Bodies at Mach 3.85. NASA TN D-284, 1960.

2. Hinson, William F.; and Falanga, Ralph A.: Effect of Jet Pluming on the Static Stability of Cone-Cylinder-Flare Configurations at a Mach Number of 9.65. NASA TN D-1352, 1962.

3. Fetterman, David E., Jr.: Effects of Simulated Rocket-Jet Exhaust on Stability and Control of a Research-Type Airplane Configuration at a Mach Number of 6.86. NASA TM X-127, 1959.

4. Falanga, Ralph A.; Hinson, William F.; and Crawford, Davis H.: Exploratory Tests of the Effects of Jet Plumes on the Flow Over Cone-Cylinder-Flare Bodies. NASA TN D-1000, 1962.

5. Stokes, George M.: Description of a 2-Foot Hypersonic Facility at the Langley Research Center. NASA TN D-939, 1961.

TABLE I.- CONFIGURATION IDENTIFICATION

Figure	Configuration	Forebody	Centerbody	Afterbody
5	111	30^{o} half-angle cone	Short	Cylinder
6 and 12	112	30^{o} half-angle cone	Short	Flare
7	113	30^{o} half-angle cone	Short	Fin
8	212	15^{o} half-angle cone	Short	Flare
9	213	15^{o} half-angle cone	Short	Fin
10	312	Ogive	Short	Flare
11	313	Ogive	Short	Fin
12	122	30^{o} half-angle cone	Long	Flare

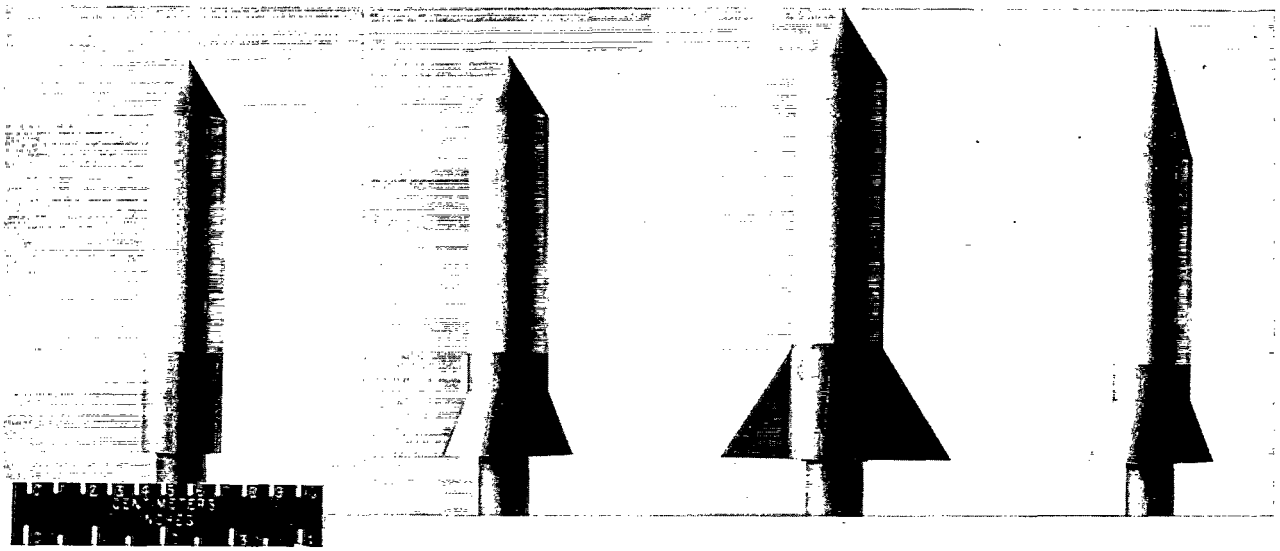

Configuration 111 Configuration 112 Configuration 113 Configuration 212

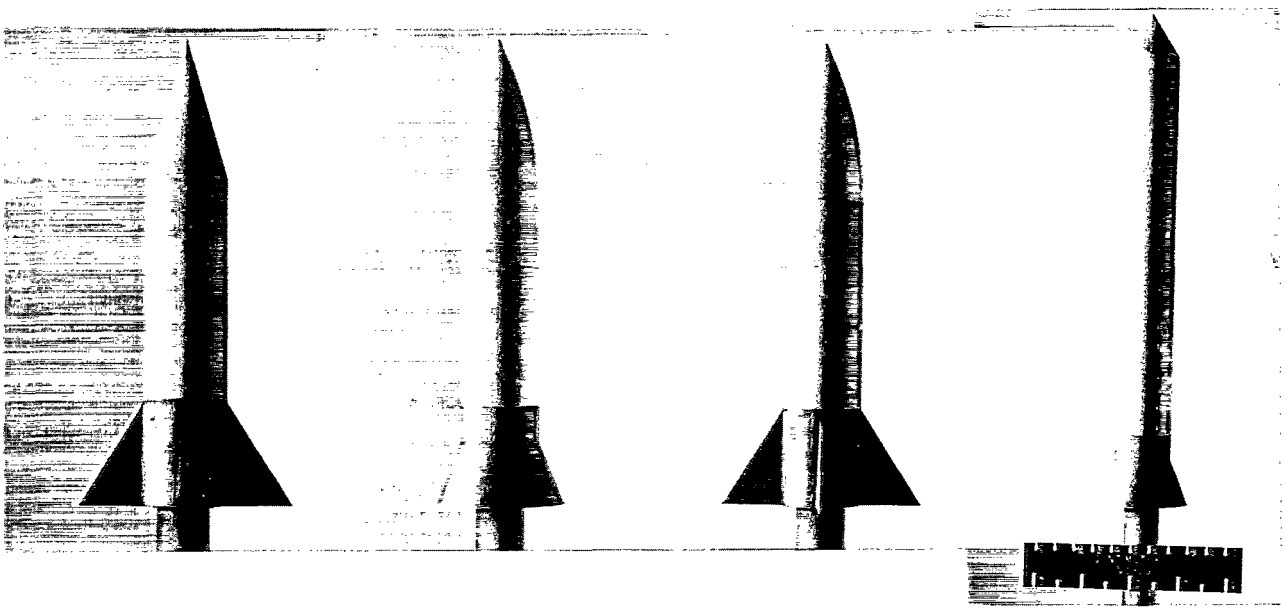

Configuration 213 Configuration 312 Configuration 313 Configuration 122

Figure 1.- Photographs of configurations tested. L-66-4534

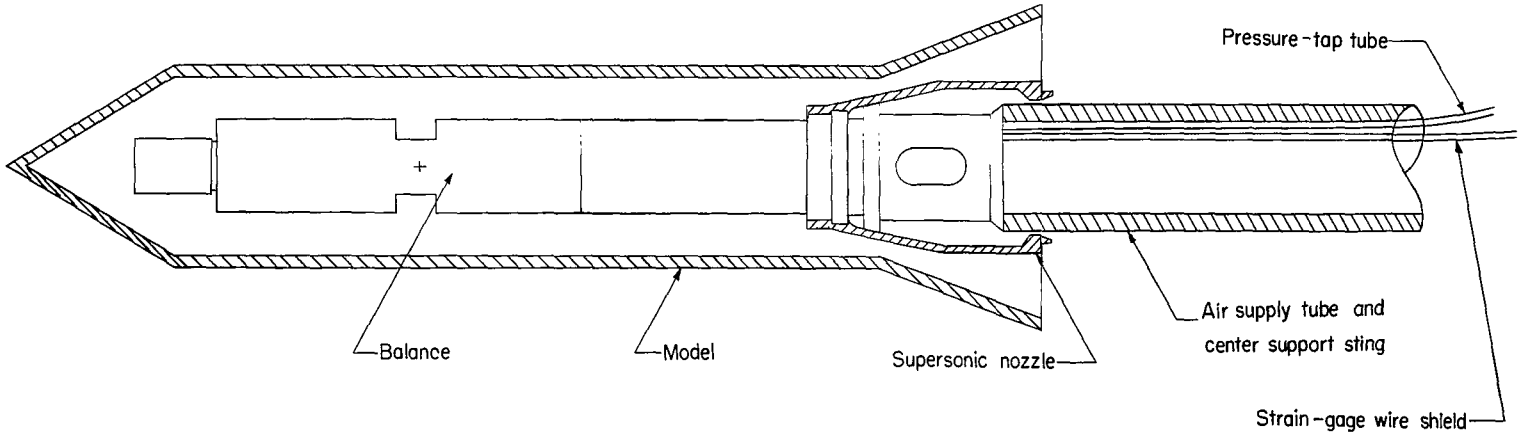

Figure 2.- Sketch of configuration 112 showing sting, balance, and nozzle arrangement.

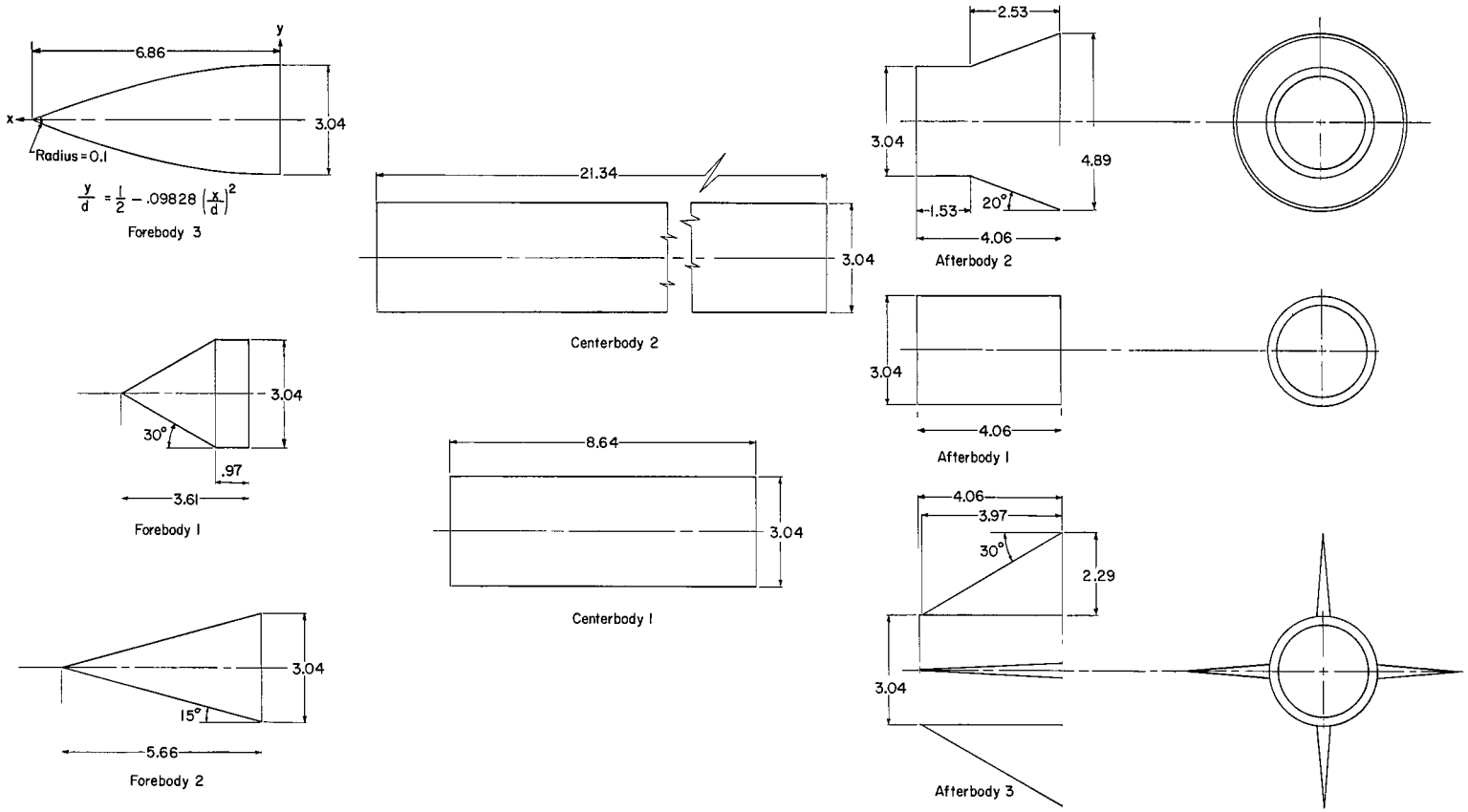

Figure 3.- Details of models tested. All dimensions are in centimeters.

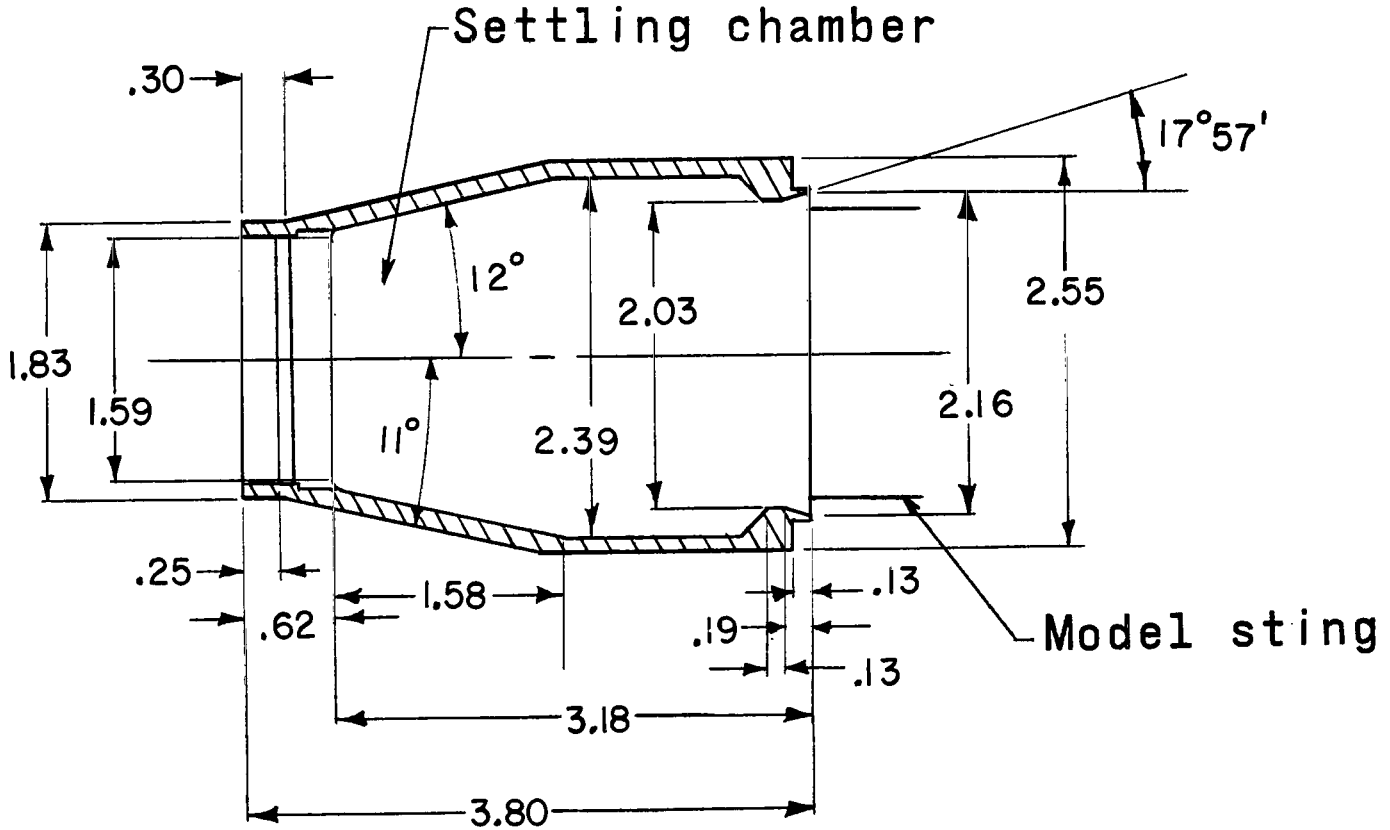

Figure 4.- Details of supersonic nozzle. All dimensions are in centimeters.

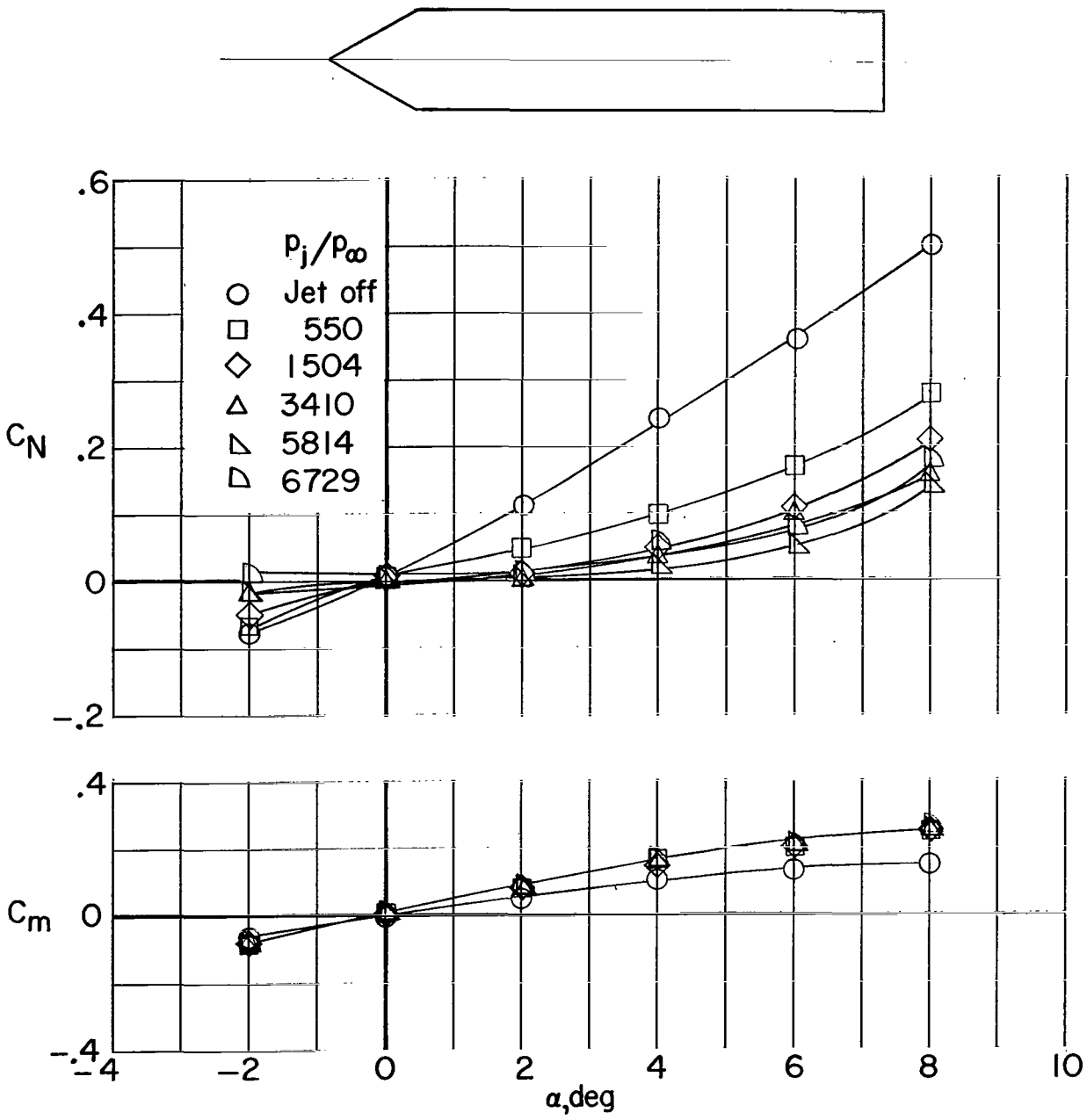

(a) C_N and C_m.

Figure 5.- Variation of C_N and C_m with angle of attack and pressure ratio p_j/p_∞ for configuration 111, including schlieren photographs.

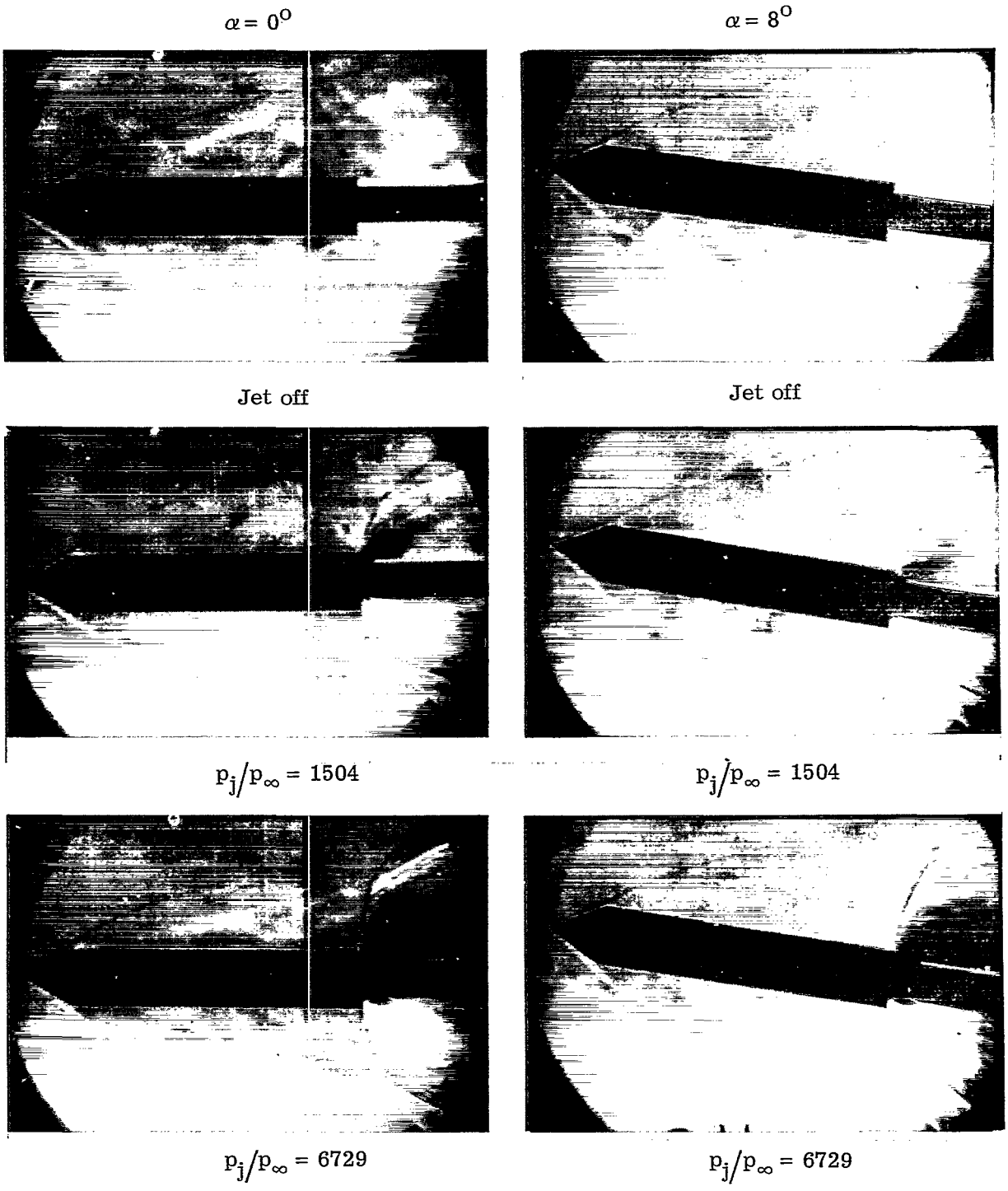

(b) Schlieren photographs. L-66-4535

Figure 5.- Concluded.

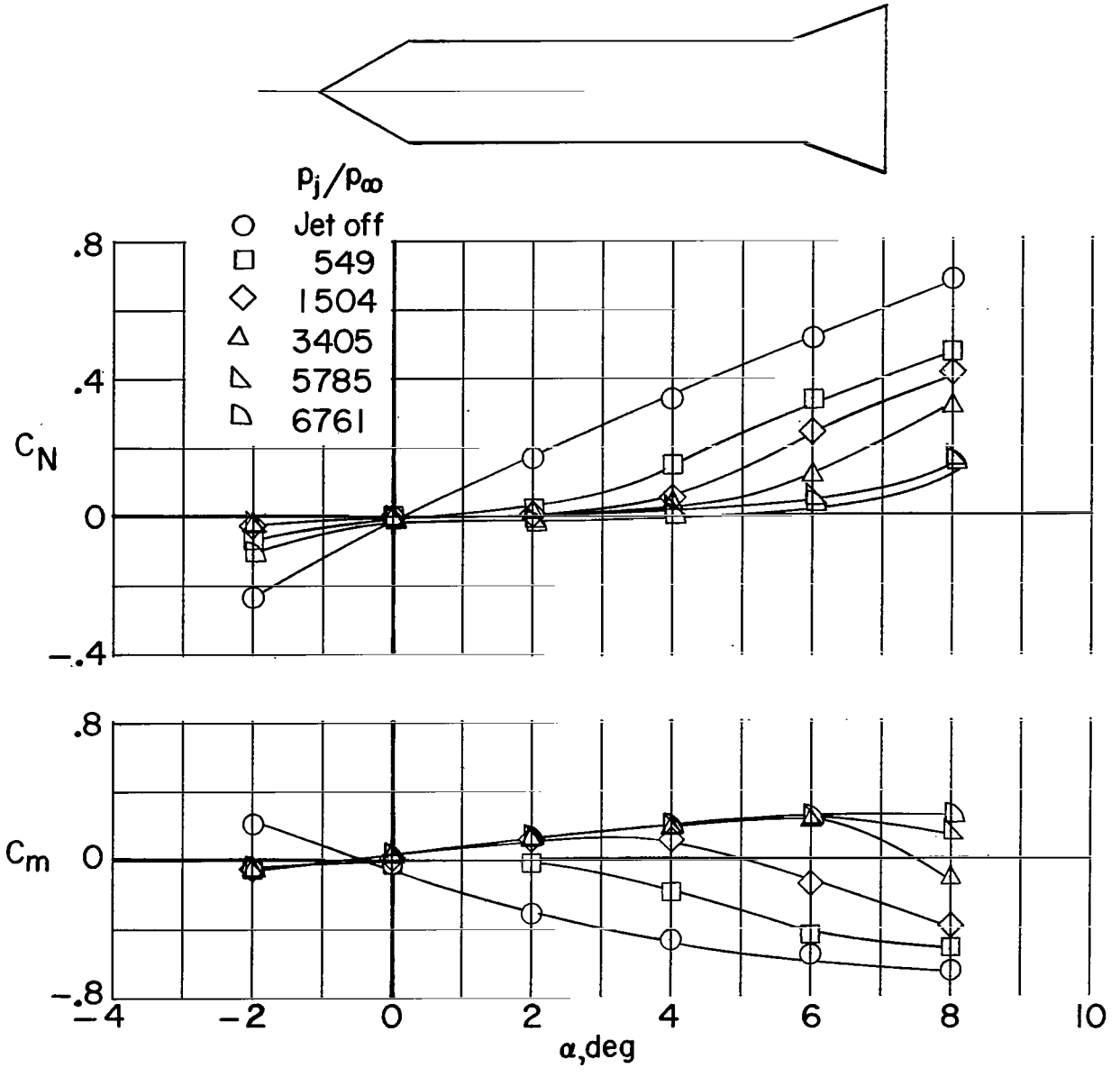

(a) C_N and C_m.

Figure 6.- Variation of C_N and C_m with angle of attack and pressure ratio p_j/p_∞ for configuration 112, including schlieren photographs.

$\alpha = 8^{o}$

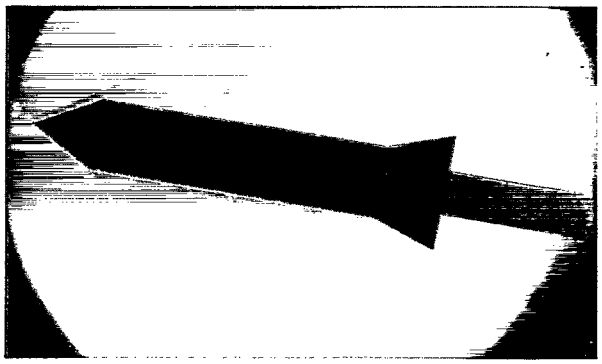

Jet off

$\alpha = 0^{o}$

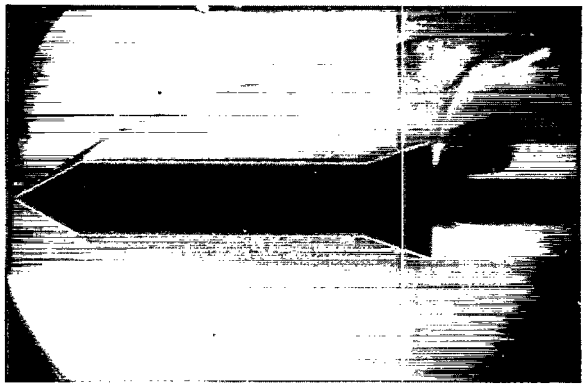

$p_j/p_\infty = 3405$

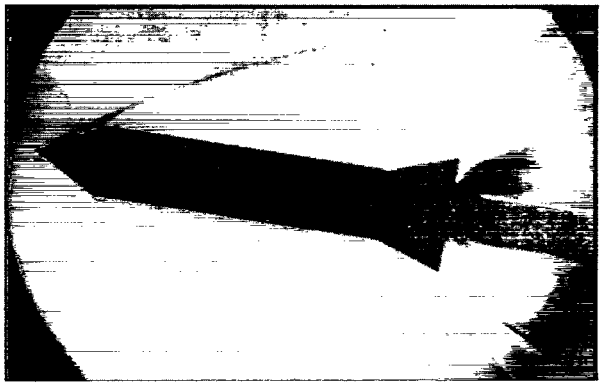

$p_j/p_\infty = 3405$

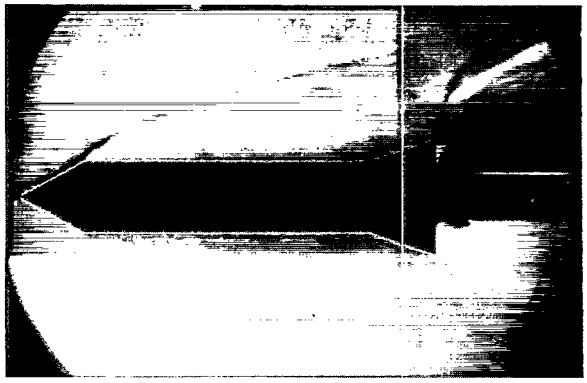

$p_j/p_\infty = 5785$

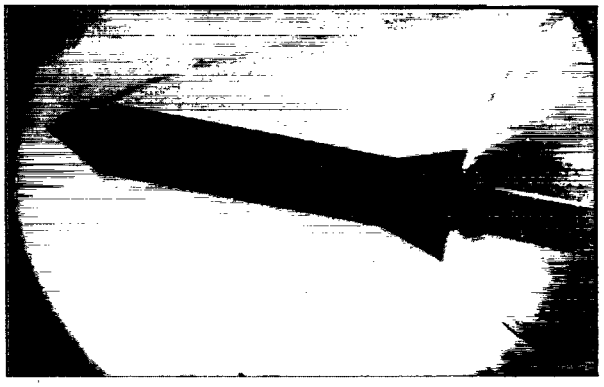

$p_j/p_\infty = 5785$

(b) Schlieren photographs.

L-66-4536

Figure 6.- Concluded.

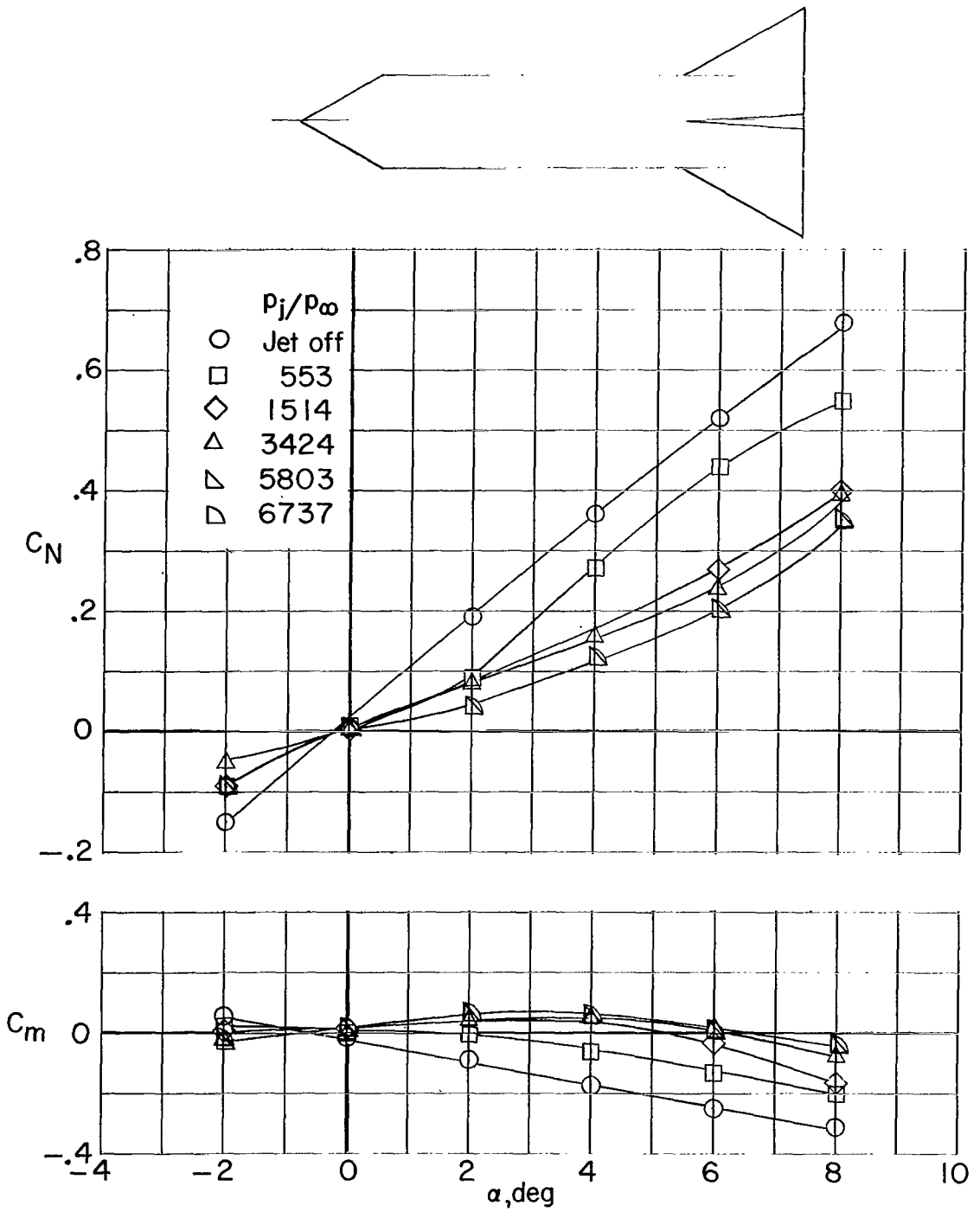

(a) C_N and C_m.

Figure 7.- Variation of C_N and C_m with angle of attack and pressure ratio p_j/p_∞ for configuration 113, including schlieren photographs.

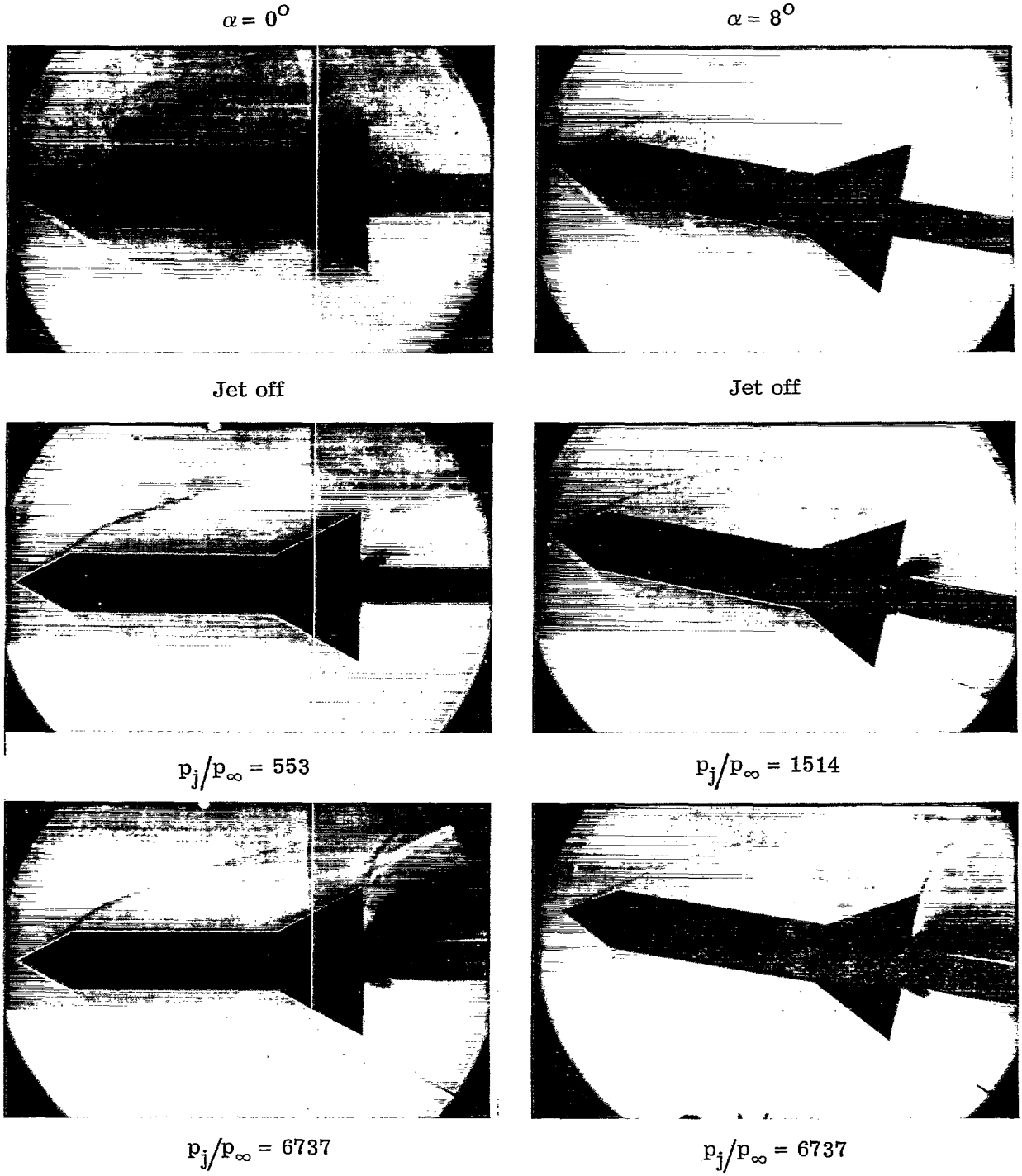

(b) Schlieren photographs. L-66-4537

Figure 7.- Concluded.

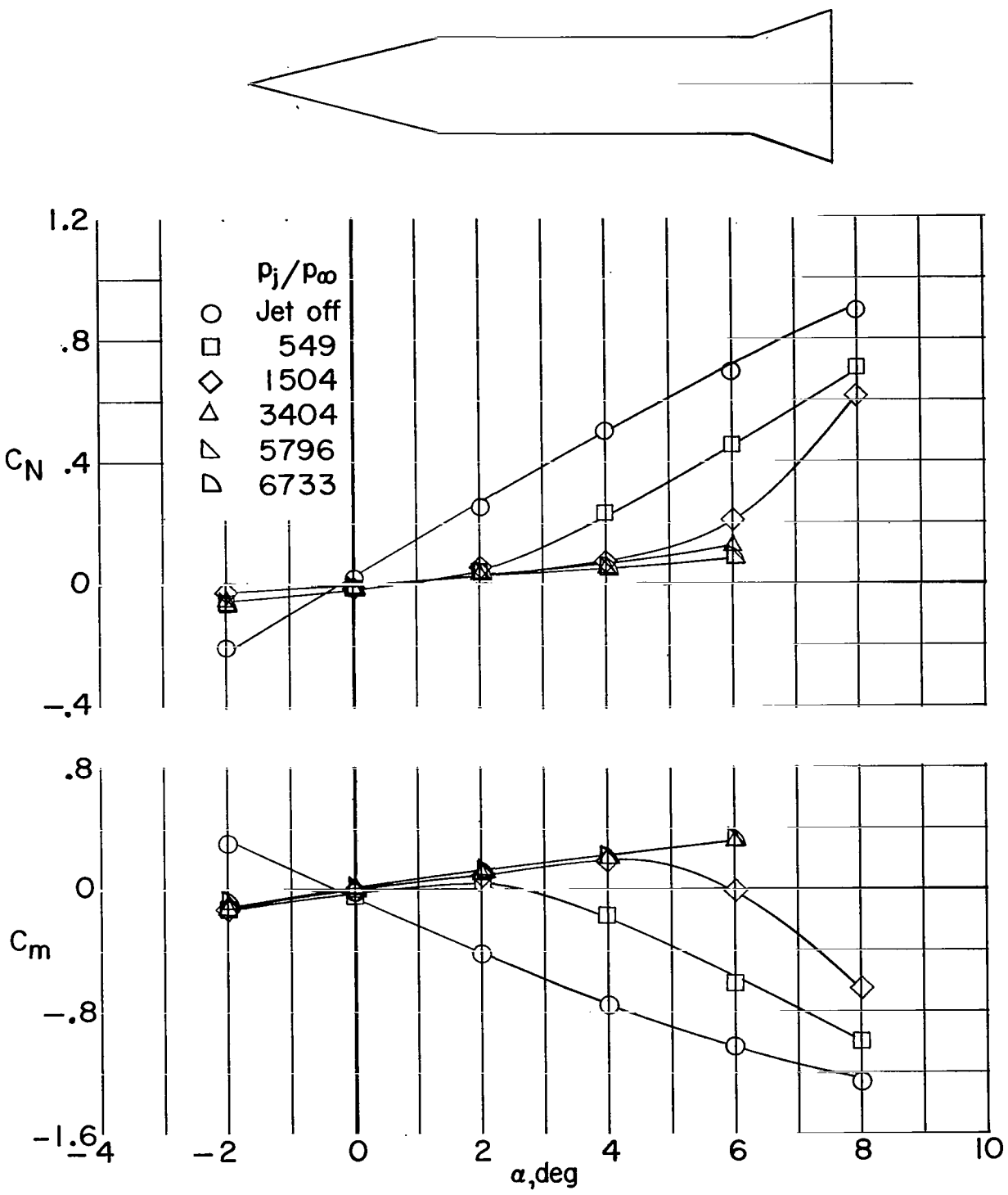

Figure 8.- Variation of C_N and C_m with angle of attack and pressure ratio p_j/p_∞ for configuration 212.

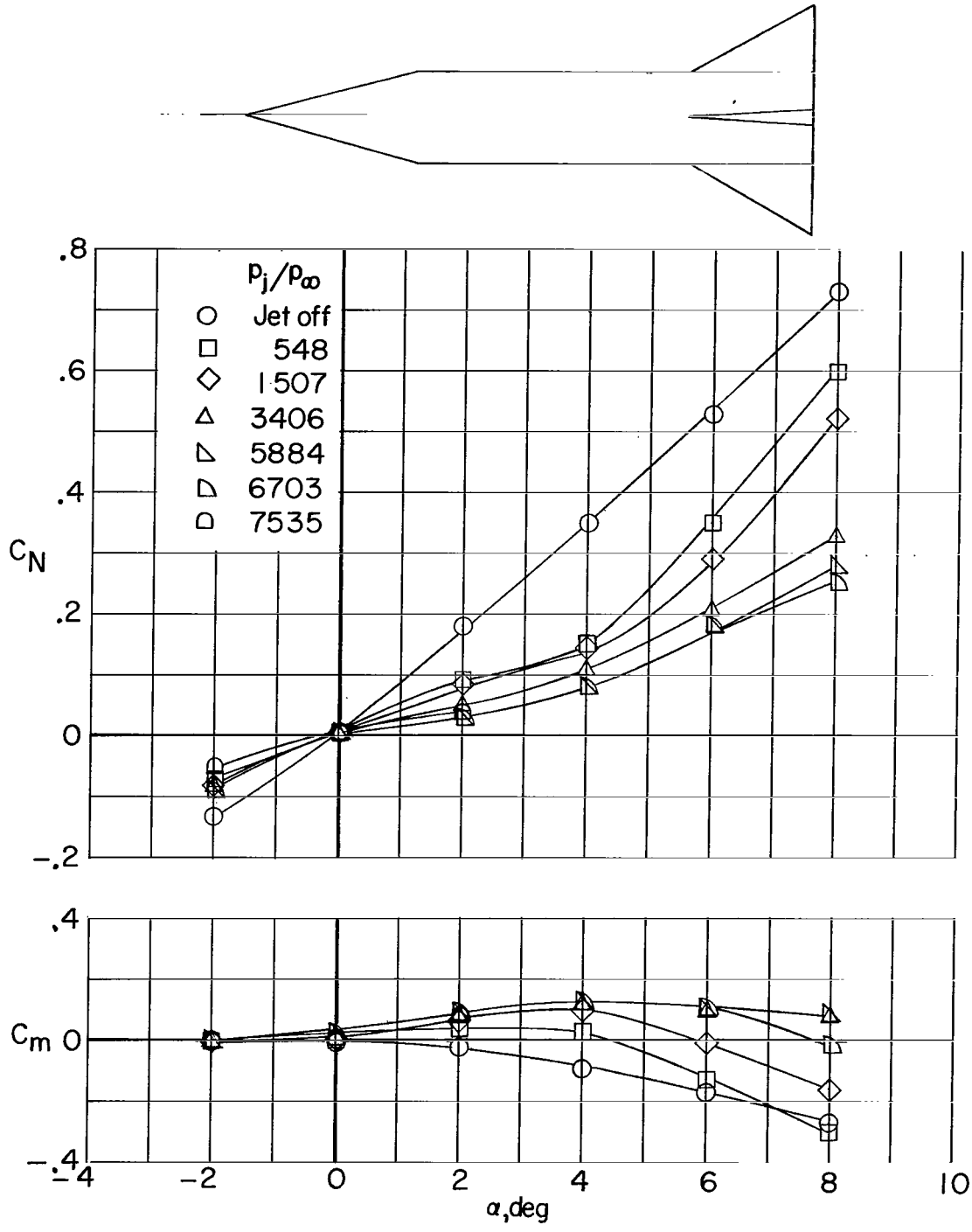

(a) C_N and C_m.

Figure 9.- Variation of C_N and C_m with angle of attack and pressure ratio p_j/p_∞ for configuration 213, including schlieren photographs.

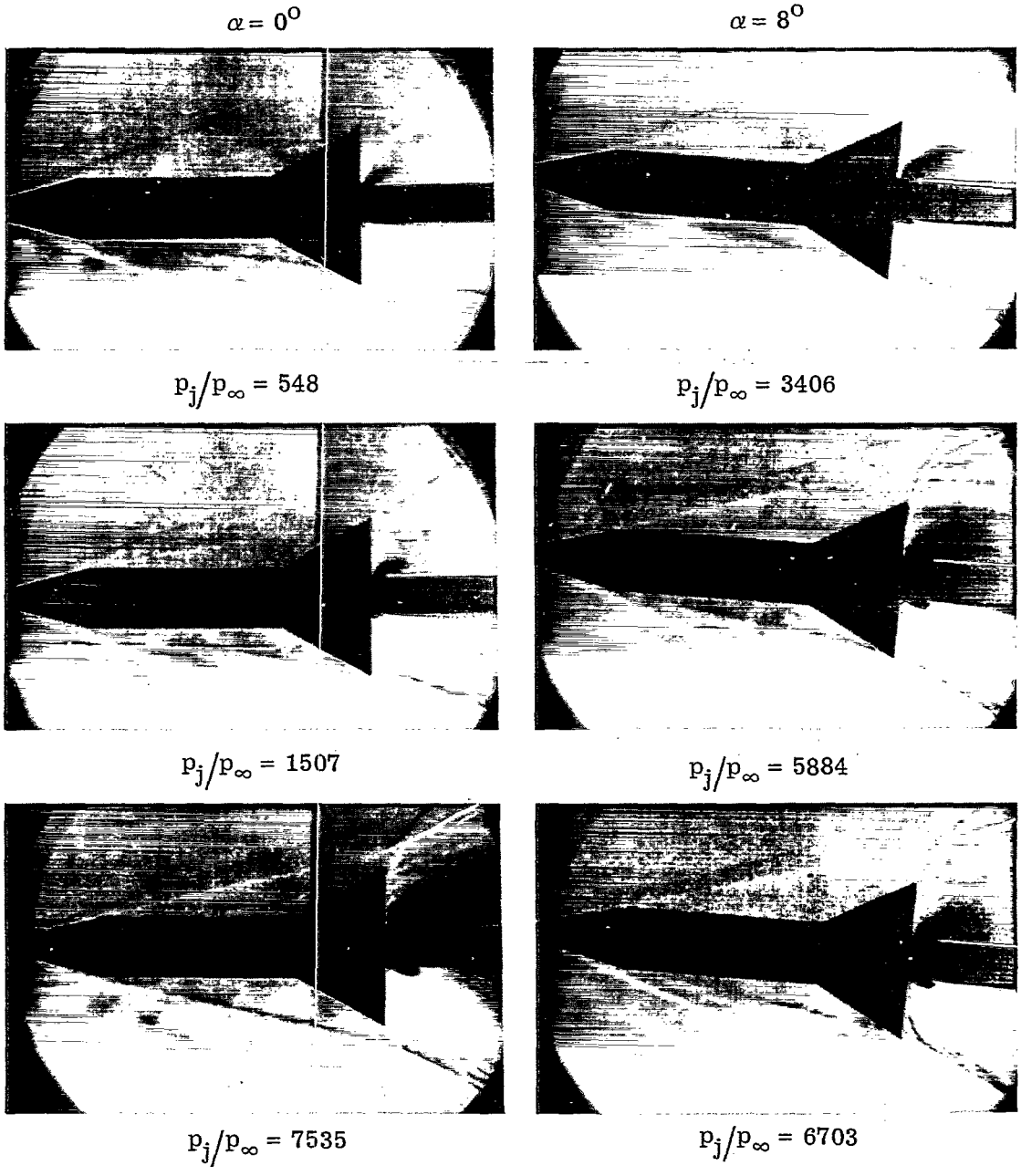

(b) Schlieren photographs. L-66-4538

Figure 9.- Concluded.

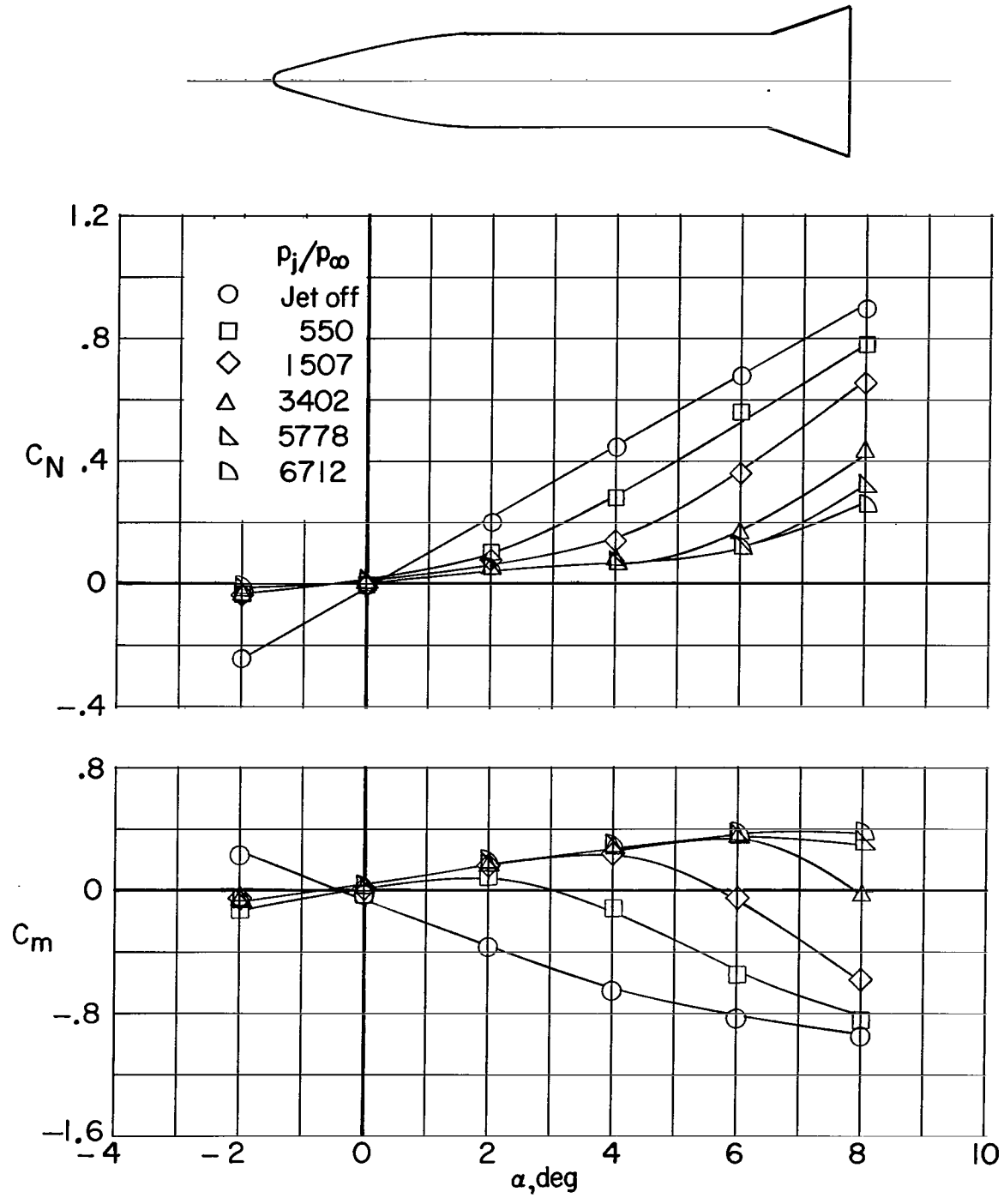

Figure 10.- Variation of C_N and C_m with angle of attack and pressure ratio p_j/p_∞ for configuration 312.

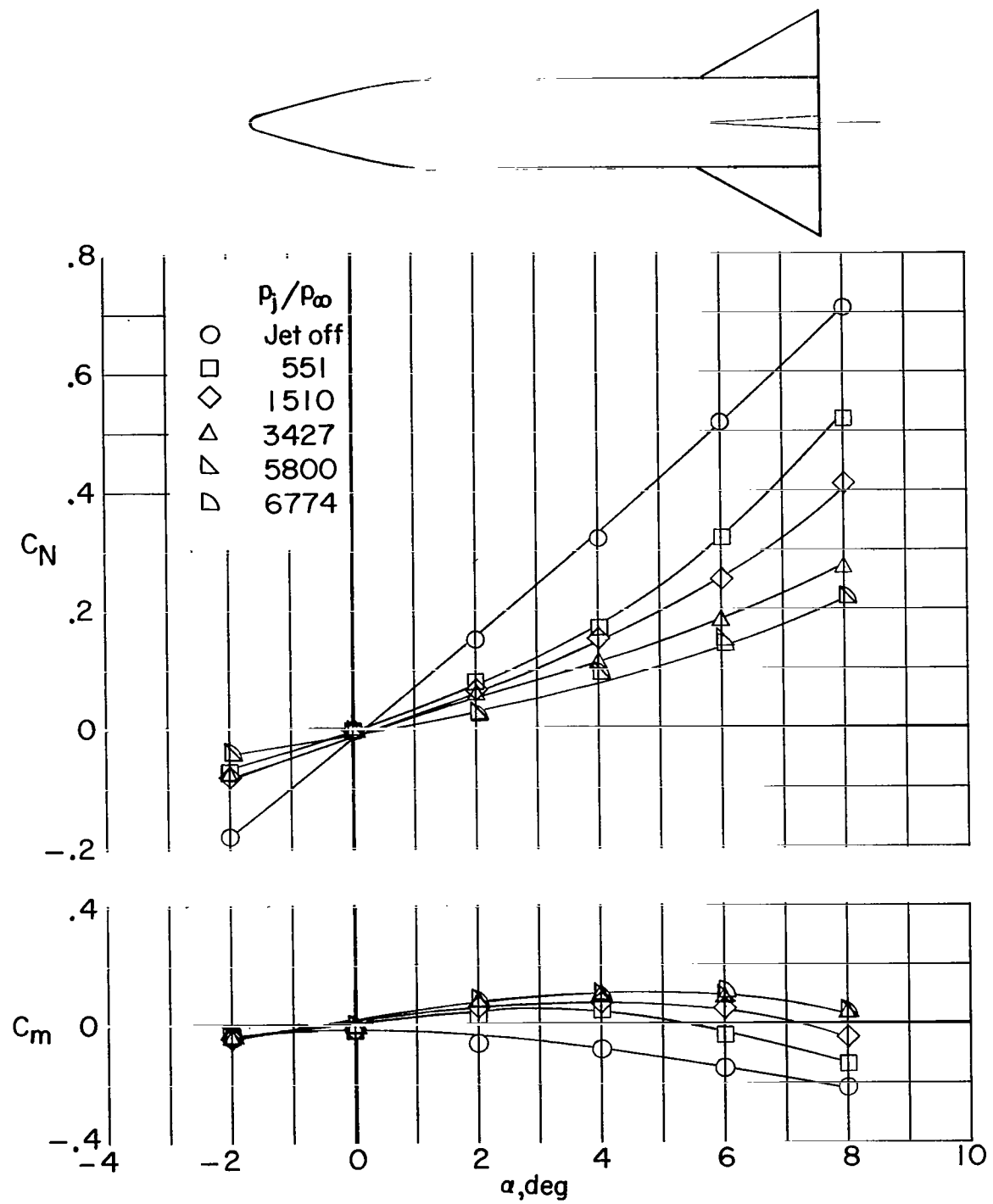

Figure 11.- Variation of C_N and C_m with angle of attack and pressure ratio p_j/p_∞ for configuration 313.

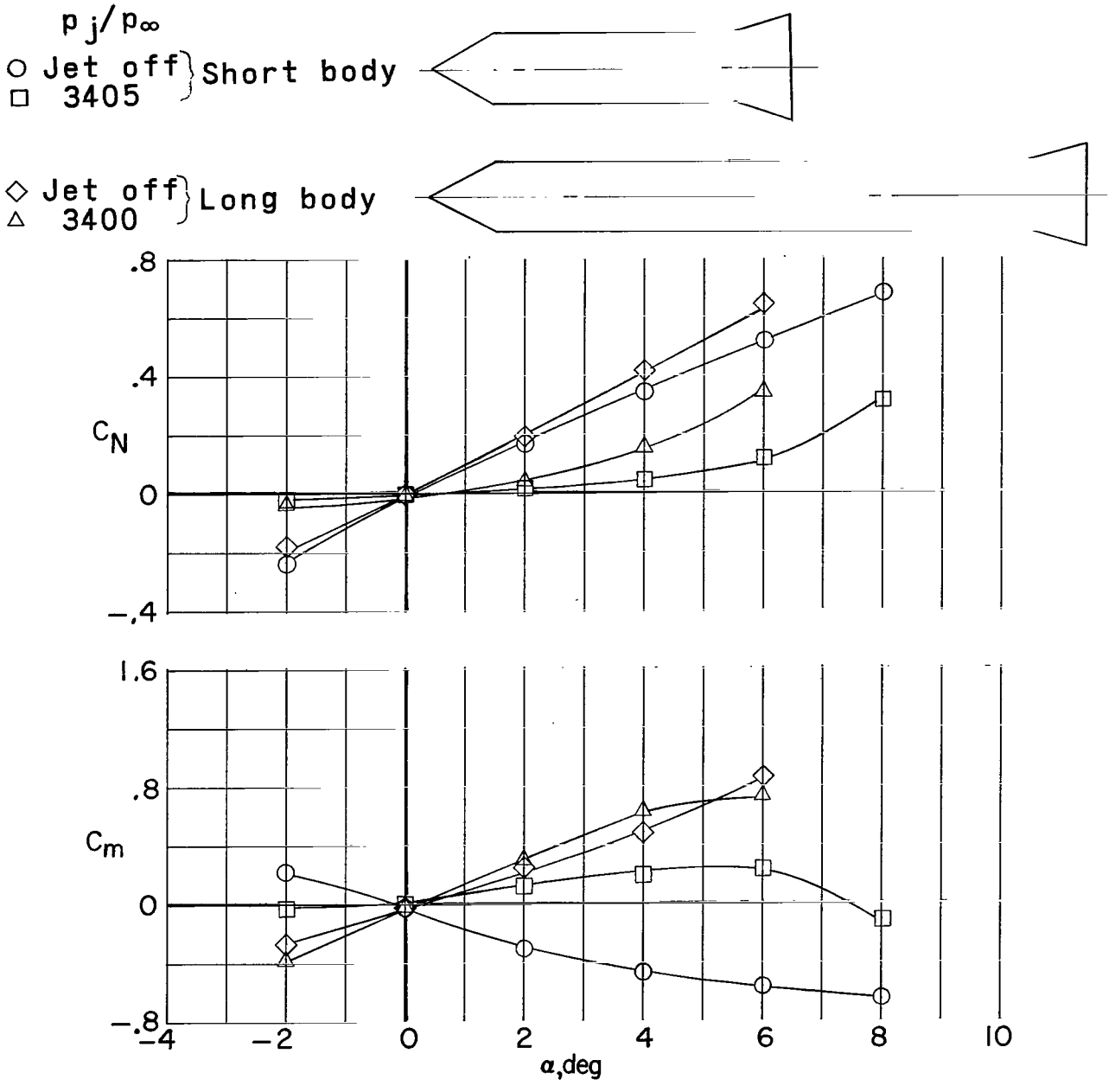

Figure 12.- Variation of C_N and C_m with angle of attack and pressure ratio p_j/p_∞ for configurations 112 (short body) and 122 (long body).

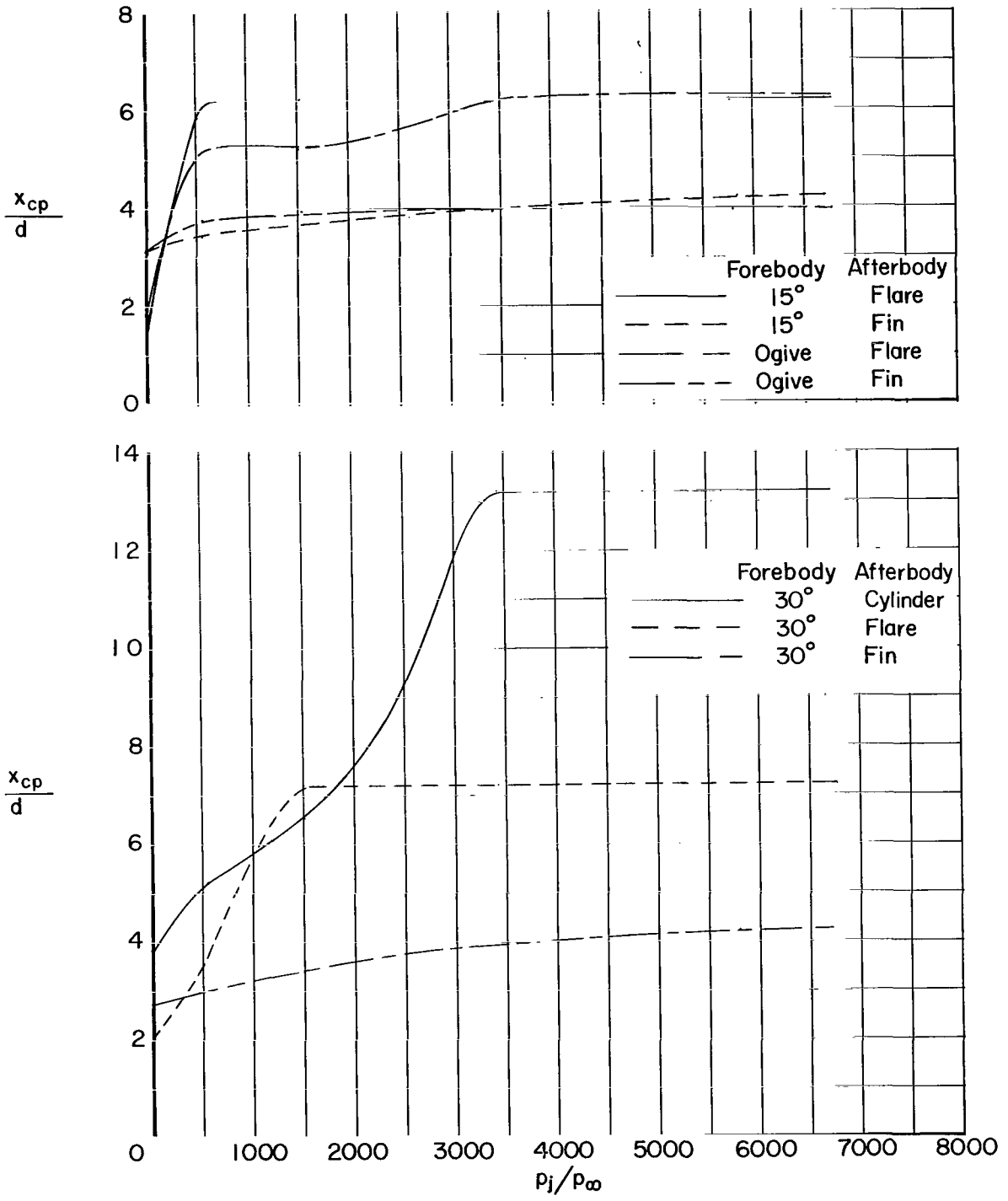

Figure 13.- Variation of x_{cp}/d with pressure ratio p_j/p_∞ for short-body configurations with various forebodies and afterbodies. $\alpha = 0^0$.

"The aeronautical and space activities of the United States shall be conducted so as to contribute . . . to the expansion of human knowledge of phenomena in the atmosphere and space. The Administration shall provide for the widest practicable and appropriate dissemination of information concerning its activities and the results thereof."

—NATIONAL AERONAUTICS AND SPACE ACT OF 1958

NASA SCIENTIFIC AND TECHNICAL PUBLICATIONS

TECHNICAL REPORTS: Scientific and technical information considered important, complete, and a lasting contribution to existing knowledge.

TECHNICAL NOTES: Information less broad in scope but nevertheless of importance as a contribution to existing knowledge.

TECHNICAL MEMORANDUMS: Information receiving limited distribution because of preliminary data, security classification, or other reasons.

CONTRACTOR REPORTS: Technical information generated in connection with a NASA contract or grant and released under NASA auspices.

TECHNICAL TRANSLATIONS: Information published in a foreign language considered to merit NASA distribution in English.

TECHNICAL REPRINTS: Information derived from NASA activities and initially published in the form of journal articles.

SPECIAL PUBLICATIONS: Information derived from or of value to NASA activities but not necessarily reporting the results of individual NASA-programmed scientific efforts. Publications include conference proceedings, monographs, data compilations, handbooks, sourcebooks, and special bibliographies.

Details on the availability of these publications may be obtained from:

SCIENTIFIC AND TECHNICAL INFORMATION DIVISION

NATIONAL AERONAUTICS AND SPACE ADMINISTRATION

Washington, D.C. 20546